All-fluorescence white organic light-emitting diodes with record-beating power efficiencies over 130 lm W^{-1} and small roll-offs

Hao Liu,[1] Yan Fu,[1] Ben Zhong Tang[1,2] and Zujin Zhao[1,*]

[1] State Key Laboratory of Luminescent Materials and Devices, Guangdong Provincial Key Laboratory of Luminescence from Molecular Aggregates, South China University of Technology, Guangzhou, 510640, China. Email: mszjzhao@scut.edu.cn.

[2] Shenzhen Institute of Aggregate Science and Technology, School of Science and Engineering, The Chinese University of Hong Kong, Shenzhen, Guangdong 518172, China.

Abstract

Improving power efficiency (*PE*) and reducing roll-off are of significant importance for the commercialization of white organic light-emitting diodes (WOLEDs) in consideration of energy conservation. Herein, record-beating *PE* of 130.7 lm W^{-1} and outstanding external quantum efficiency (*EQE*) of 31.1% are achieved in all-fluorescence two-color WOLEDs based on a simple sandwich configuration of emitting layer consisting of sky-blue and orange delayed fluorescence materials. By introducing a red fluorescence dopant, all-fluorescence three-color WOLEDs with high color rendering index are constructed based on an out-of-phase sensitization configuration, furnishing ultrahigh *PE* of 106.8 lm W^{-1} and *EQE* of 30.8%. More importantly, both two-color and three-color WOLEDs maintain excellent *PE*s at operating luminance with smaller roll-offs than the reported state-of-the-art WOLEDs, and further device optimization realizes outstanding comprehensive performances of low driving voltages, large luminance, high *PE*s and long operational lifetimes. The underlying mechanisms of the impressive performances are elucidated by host-tuning effect and electron-trapping effect, providing useful guidance for the development of energy-conserving all-fluorescence WOLEDs.

Introduction

White organic light-emitting diodes (WOLEDs) are emerged as the core for the next-generation display and illumination devices, and substantial efforts have been devoted to functional materials exploration, exciton manipulation and distribution, configuration optimization and fabrication technique development.[1-3] To achieve high electroluminescence (EL) efficiencies, all-phosphorescence systems and fluorescence-phosphorescence hybrid systems are widely studied in reported WOLEDs due to the high exciton utilization efficiencies of phosphorescence materials. But the high cost of noble metal-containing phosphorescence materials as well as the lack of robust blue phosphorescence materials impede the widespread commercialization of WOLEDs to a large degree. Purely organic thermally activated delayed fluorescence (TADF) materials can theoretically harness 100% electrogenerated excitons through reverse intersystem crossing (RISC) from the lowest triplet excited (T_1) state to the lowest singlet excited (S_1) state based on a small energy gap (ΔE_{ST}) between S_1 and T_1 states,[4-7] and thus have been regarded as the successors of phosphorescence materials. The external quantum efficiency (*EQE*) of monochromatic OLEDs based on TADF emitters have successfully surpassed 30%, and even approached 40% in very recent reports.[8-12] Therefore, certain high-efficiency TADF emitters with competitive prices hold great potentials to replace phosphorescence materials in OLED industry.

On the other hand, TADF materials are generally designed to have highly twisted electron donor-acceptor (D-A) structures to acquire small ΔE_{ST}s. Such kind of twisted D-A structures can also endow the molecules with ambipolar carrier transport ability, which is favorable for achieving carrier balance and thus high exciton

recombination efficiencies in devices. Therefore, TADF materials can behavior as hosts as well as sensitizers for various kinds of luminescent materials to greatly improve device performances because of enhanced efficiencies for exciton production and utilization.[13-17] The conventional fluorescence emitters, who can only harness singlet excitons, particularly benefit from doping in TADF materials, rendering much higher EL efficiencies than those in common host materials. Combining the high color purity and stability of fluorescence emitters, all-fluorescence WOLEDs using TADF materials as both hosts and sensitizers possess superior competitiveness and merits to conventional all-fluorescence WOLEDs based on common fluorescence emitters, bringing about new opportunities for the advancement of WOLEDs.[18-24]

For white light illumination, power conservation is a vital index for WOLEDs, which can be reflected by the power efficiency (*PE*). And the *PE* at operating luminance is a more accurate parameter for the evaluation of WOLED performances. However, most of the efficient WOLEDs encounter sharp declines in *PE*s at high luminance, and effective approaches to improve *PE*s and reduce *PE* roll-offs are received relatively less attention. The exciton utilization of the emitters and the carrier injection and transport of the devices play critical roles in determining *PE*s, which should be carefully addressed in the design of energy-conserving WOLEDs by properly selecting not only luminescent materials but also host materials. Currently, several new hosts are demonstrated to be promising candidates for WOLEDs. Organic semiconductors generally exhibit asymmetric carrier transport property, in which the mobility of holes is generally much faster than electrons.[25] The n-type hosts with high T_1 energy levels can erase the barrier of electron injection and balance the transports of electrons and holes, which is conducive to lowering driving voltages of the devices (Fig. 1a).[26] However, such kind of n-type hosts are difficult to design, and there are only very limited cases of n-type hosts successfully applied in WOLEDs to boost *PE*s. Besides, intermolecular charge transfer host, namely exciplex host, is reported as an effective alternative for solving the power consumption problem, because their ambipolar carrier transport and easy carrier injection can ensure smooth recombination of excitons in emitting layer (EML), rendering low turn-on voltages for WOLEDs.[27-30] Nevertheless, the fabrication complexity involving multielement doping technique often results in failure to acquire desired device performances based on exciplex host. The application of TADF materials as hosts is another promising avenue to enhance *PE*s owing to their narrower energy gaps compared with conventional hosts as well as much better exciton harvesting ability.[24] The ideal multifunctional TADF materials for both hosts and emitters require not only balanced ambipolar carrier transport but also suppressed exciton annihilation and emission quenching in neat films, which is challenging because most reported TADF materials suffer from serious losses of emission and exciton in neat films, and thus have to be doped in other conventional hosts when applied in OLEDs. In consequence, up to now, the successful cases of high-performances WOLEDs based on TADF materials with comparable or superior *PE*s to those of the best phosphorescence materials engaged WOLEDs are extremely rare.[30-32]

In our previous work, a robust sky-blue delayed fluorescence molecule, (4-(spiro[acridine-9,9'-fluoren]-10-yl)phenyl)(9-(3,5-di(carbazol-9-yl)phenyl)carbazol-3-yl)methanone (TCP-BP-SFAC), with balanced ambipolar carrier transport and excellent PL efficiency in neat film was created, which provided record-high *EQE*s of 26.1% and 38.6% in nondoped and doped OLEDs, respectively.[10] These intriguing properties enable TCP-BP-SFAC to function as host and emitter simultaneously in WOLEDs. In this contribution, a simple sandwich configuration consisting of an orange EML located between two sky-blue EMLs is proposed to boost the EL efficiencies of all-fluorescence two-color WOLEDs (Fig. 1a), in which the neat film of TCP-BP-SFAC (Fig. 1b) is adopted as sky-blue EML, and the doped film of an efficient orange TADF emitter 2,3,5,6-tetrakis(3,6-di-(*tert*-butyl)carbazol-9-yl)-1,4-dicyanobenzene (4CzTPNBu) blended in TCP-BP-SFAC host functions as orange EML. The sandwich configuration effectively alleviates exciton quenching caused by the electron-trapping effect of 4CzTPNBu. Thanks to the balanced ambipolar transportation and high solid-state efficiency of TCP-BP-SFAC, the record-beating *PE* of 130.7 lm W^{-1} is successfully achieved in all-fluorescence two-color warm-white devices. For further improving the color quality, a

red EML comprised of a red fluorescence dopant 5,10,15,20-tetraphenylbisbenz[5,6]indeno[1,2,3-cd:1′,2′,3′-lm]perylene (DBP) doped in TCP-BP-SFAC host is introduced, which is sensitized by an efficient out-of-phase configuration via Förster energy transfer (FET) as shown in Fig. 1a. The all-fluorescence three-color WOLEDs achieve nearly the same *EQE*s of 30.8% as two-color devices, as well as high *PE*s over 106 lm W^{-1}, which are also pioneering among all-fluorescence three-color WOLEDs reported so far. Importantly, the *PE*s at operating luminance of 100 and 1000 cd m^{-2} are kept at satisfactory levels for both two-color and three-color devices, indicating they are practicable devices for illumination. The in-depth working mechanisms behind these devices are thoroughly studied and the effective design strategy for high-performance all-fluorescence WOLEDs is elucidated in detail, in consideration of the electron- trapping effect and host-tuning effect. Moreover, the operational lifetimes to 50% (LT_{50}) at the initial luminance of 100 cd m^{-2} reach over 50000 h, validating the presented design strategies for all-fluorescence WOLEDs are of high potential for practial application.

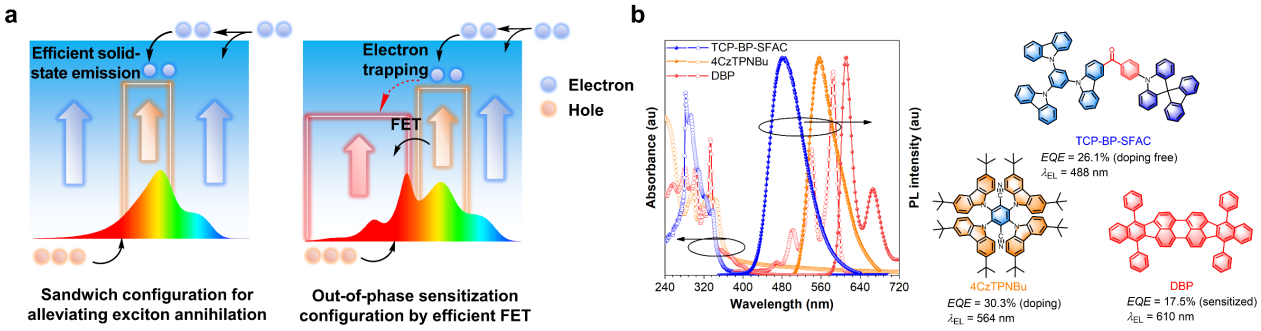

Fig. 1 a Schemical mechanisms of sandwich configuration design and out-of-phase sensitizating system. **b** Molecular structures, and absorption and photoluminescence (PL) spectra of sky-blue emitter TCP-BP-SFAC, orange emitter 4CzTPNBu and red emitter DBP applied in all-fluorescence two-color and three-color WOLEDs in this work.

Results

All-fluorescence two-color WOLEDs

The basic device configuration for all-fluorescence two-color WOLEDs is designed as ITO/HATCN (5 nm)/TAPC (50 nm)/TCTA (5 nm)/mCP (5 nm)/EML/PPF (5 nm)/TmPyPB (40 nm)/LiF (1 nm)/Al, in which indium tin oxide (ITO) is transparent anode, dipyrazino[2,3-f:2′,3′-h]quinoxaline-2,3,6,7,10,11-hexacarbonitrile (HATCN) is hole injection layer, 4,4'-cyclohexylidenebis[*N*,*N*-bis(4-methylphenyl)aniline] (TAPC) is hole-transporting layer, tris[4-(carbazol-9-yl)phenyl]amine (TCTA) functions not only as hole-transporting layer but also electron-blocking layer, 1,3-bis(carbazol-9-yl)benzene (mCP) works as buffer layer between hole-transporting layer and EML in view of its high T_1 energy level, 2,8-bis(diphenyl-phosphoryl)-dibenzo[b,d]furan (PPF) is exciton-blocking layer, 1,3,5-tri(m-pyrid-3-yl-phenyl)benzene (TmPyPB) is electron-transporting layer, and LiF/Al works as cathode (Supplementary Table 1). A blue-orange-blue sandwich configuration is designed for EML responsible for white EL emission, comprised of TCP-BP-SFAC (15 – *x* nm)/1.5 wt% 4CzTPNBu: TCP-BP-SFAC (5 nm)/TCP-BP-SFAC (*x* nm) (Fig. 2a), in which *x* = 0~8 by the step of 1 nm, corresponding to devices W1-0 to W1-8. The key parameters of devices W1-0~W1-8 are shown in Fig. 2c, d, e, Supplementary Fig. 1 and Table 1. All the devices can be turned on at low voltages of ~2.6 V and exhibit a low operational voltage of ~3.2 V at luminance of 1000 cd m^{-2}. Initially, the EL efficiencies are gradually enhanced along with the increase of *x* and achieve maximum at *x* = 6. Further increasing *x* leads to slight decrease in EL efficiencies. The best device W1-6 radiates intense warm-white light with a maximum luminance (L_{max}) of 52690 cd m^{-2}, and provides significantly boosted *PE* of 130.7 lm W^{-1} in comparison with those of the reported WOLEDs (< 110 lm W^{-1}) (Fig. 2e and Supplementary Table 2).[23,24,29-32] The efficiency distribution of 25 devices with the identical configuration of W1-6 verifies the good repeatability (Fig. 2f). The roll-offs of *PE*s and *EQE*s of all the devices are very small at working luminance. The maximum *EQE* is 31.1%, which

is kept as 29.7% and 25.3% at luminance of 100 cd m^{-2} and 1000 cd m^{-2}, respectively. More importantly, outstanding *PE*s are achieved as 108.8 lm W^{-1} and 83.5 lm W^{-1} at luminance of 100 cd m^{-2} and 1000 cd m^{-2}, respectively, much better than those of the reported state-of-the-art WOLEDs.[23,24,29-32] The remarkably high *PE*s at working luminance demonstrate the realization of energy conservation of the devices, which makes them more applicable and competitive in practical use.

In order to understand the impressive EL performance, comprehensive researches on the working mechanism of these devices are conducted. Device W1-0 can be regarded as a dual emissive layer device, whose EL efficiencies

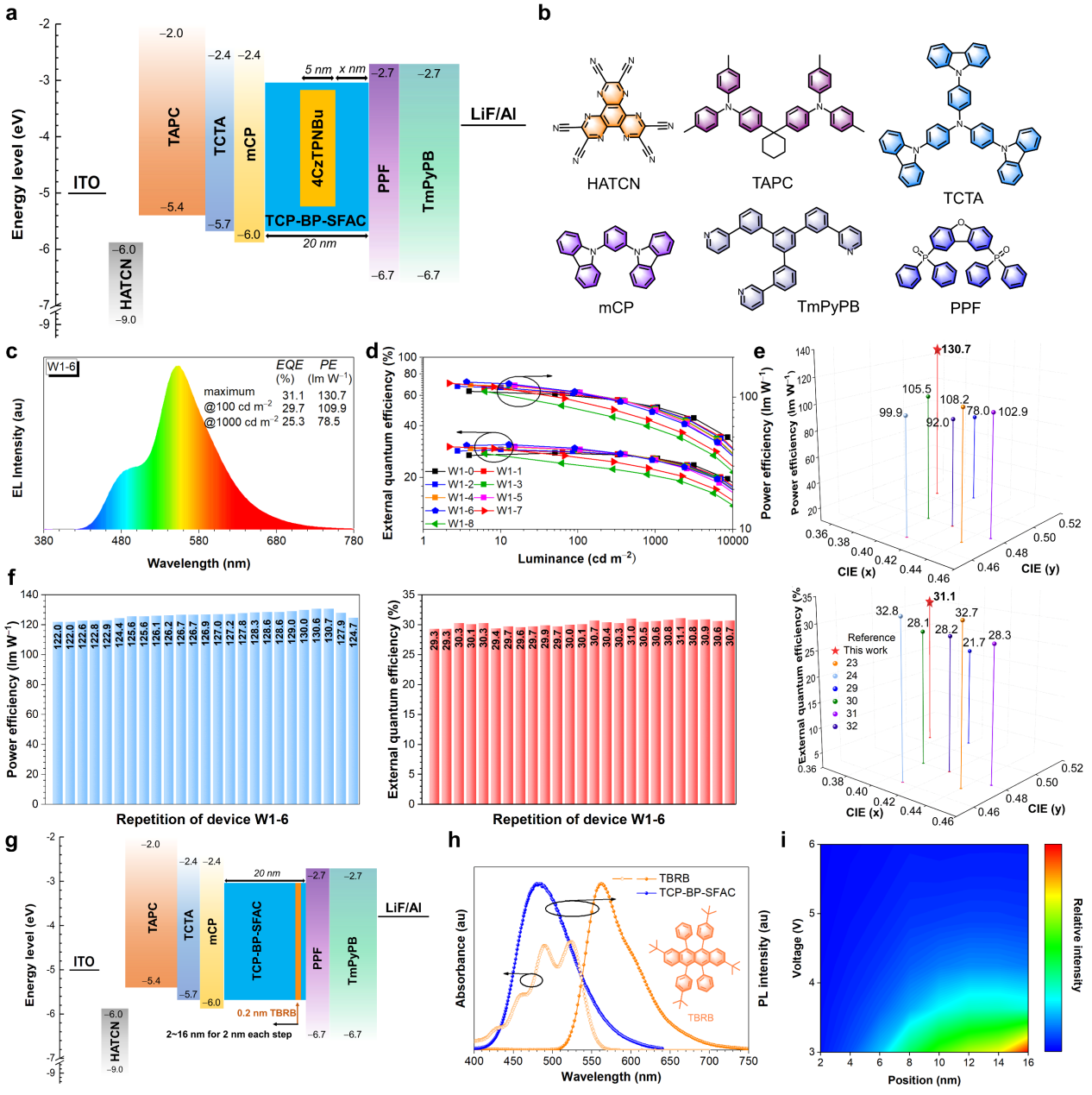

Fig. 2 **a** Device configuration of all-fluorescence two-color WOLEDs. **b** Molecular structures of the functional materials applied in WOLEDs. **c** EL spectra of device W1-6. **d** External quantum efficiency-luminance-power efficiency curves of device W1-0~W1-8. **e** External quantum efficiency and power efficiency of representative two-color WOLEDs versus CIE coordinates. **f** Summary of power efficiency and external quantum efficiency of 25 devices based on the configuration of W1-6. **g** Device configuration for exciton recombination zone detecting. **h** Absorption and PL spectra of TCP-BP-SFAC in neat film) and TBRB in toluene solution. **i** Relative intensity of TBRB detector versus position and voltage.

are even lower than those of the reported monochromatic OLEDs based on 4CzTPNBu, implying there is energy loss in W1-0. The single carrier devices of the neat film of TCP-BP-SFAC and doped film of 1.5 wt% 4CzTPNBu: TCP-BP-SFAC disclose that 4CzTPNBu has neglectable hole-trapping effect but significant electron-trapping effect in TCP-BP-SFAC host (Supplementary Fig. 2). In that case, the exciton recombination zone in W1-0 will be greatly constrained in a narrow zone in orange EML (Supplementary Fig. 3), which induces unnecessary energy loss due to triplet-triplet annihilation and triplet-singlet annihilation.[33] By increasing the thickness of TCP-BP-SFAC layer adjacent to PPF layer, the excitons can partly recombine during electron shifting to 4CzTPNBu. Thereby, the excitons can be distributed in a dispersed manner in a wide zone, which alleviates exciton quenching caused by accumulation as depicted in Fig. 1a. The appropriate frontier molecular orbitals of TCP-BP-SFAC also bring about low turn-on voltages comparable with those of WOLEDs based on exciplex hosts.[29] The EL efficiencies tend to decline by continuously increasing the thickness of TCP-BP-SFAC layer (x = 7 and 8), because the orange EML gets too far away to harvest sufficient excitons and many excitons are recombined in TCP-BP-SFAC layer as depicted in the EL spectra (Supplementary Fig. 1). The EL efficiency of TCP-BP-SFAC in neat film is lower than that of 4CzTPNBu in doped film, which is probably responsible for the efficiency decline in devices W1-7 and W1-8.

Moreover, an orange fluorescence emitter TBRB is used as detector to study the FET process in the device (Fig. 2g). The absorption spectrum of TBRB is finely overlapped with the PL spectrum of TCP-BP-SFAC (Fig. 2h), indicating sufficient FET can happen from TCP-BP-SFAC to TBRB. An ultrathin (0.2 nm) layer of TBRB neat film is inserted into the TCP-BP-SFAC layer at varied positions, and the relative emission intensity of TBRB/TCP-BP-SFAC is recorded to draw the relative intensity-position-voltage graph (Fig. 2i). It is found that the exciton recombination zone tends to locate near the hole-transporting part at low voltages, but is more evenly distributed over the entire EML at high voltages. Therefore, it is deduced that the electrons can arrive at 4CzTPNBu at low voltages with partial recombination in TCP-BP-SFAC layer, and shift towards another TCP-BP-SFAC layer through 4CzTPNBu when the operating voltage is increased, leading to enhanced blue component in white light. So, the

Table 1. EL performance of two-color all-fluorescence WOLEDs

Device	Voltage (V) [a]	*CE* (cd A^{-1}) [b]	*PE* (lm W^{-1}) [b]	*EQE* (%) [b]	CIE (x,y) [c]	L_{max}
	V_{on}/100/1000 cd m^{-2}	max/100/1000 cd m^{-2}	max/100/1000 cd m^{-2}	max/100/1000 cd m^{-2}		(cd m^{-2}) [d]
W1-0	2.6/2.9/3.5	93.7/92.6/75.3	111.0/103.1/67.6	27.7/27.6/24.1	(0.355, 0.510)	36410
W1-1	2.5/2.9/3.2	96.9/94.6/85.0	117.0/105.2/83.5	28.8/28.2/25.8	(0.416, 0.531)	51570
W1-2	2.5/2.8/3.2	95.8/94.7/83.9	120.4/105.9/82.4	29.1/28.3/25.6	(0.415, 0.529)	51670
W1-3	2.5/2.8/3.2	101.4/97.0/82.9	122.5/108.8/81.4	30.0/29.0/25.7	(0.403, 0.522)	48350
W1-4	2.5/2.8/3.2	100.3/96.2/81.8	121.2/108.0/80.3	30.0/29.0/25.5	(0.405, 0.521)	50530
W1-5	2.5/2.8/3.2	101.5/96.7/80.5	122.6/108.5/79.0	30.2/29.1/25.1	(0.396, 0.519)	51310
W1-6	2.5/2.8/3.2	104.2/98.0/78.9	130.7/109.9/78.5	31.1/29.7/25.3	(0.374, 0.505)	52690
W1-7	2.5/2.9/3.2	101.4/85.8/68.5	127.4/95.3/67.2	30.2/26.5/22.7	(0.342, 0.492)	45550
W1-8	2.5/2.9/3.2	91.4/75.4/61.5	110.4/83.8/60.4	27.5/23.9/20.9	(0.323, 0.482)	44010
W2-1	2.5/2.9/3.4	85.0/73.0/56.2	106.8/80.6/52.6	30.8/26.4/20.6	(0.394, 0.476)	42410
W2-2	2.5/2.9/3.4	80.1/75.2/61.7	99.7/83.0/58.2	29.1/27.2/22.4	(0.415, 0.482)	48250
W2-3	2.5/2.9/3.4	73.5/66.2/52.2	92.4/72.8/48.2	29.6/25.9/20.0	(0.415, 0.469)	41380
W3-1	2.4/2.8/3.3	79.5/78.1/69.1	101.7/87.6/66.4	26.0/24.1/21.3	(0.435, 0.514)	99690
W3-2	2.4/3.0/3.5	75.7/72.3/63.2	97.5/75.7/56.8	24.3/23.2/20.4	(0.452, 0.509)	95670
W3-3	2.4/2.8/3.5	62.9/53.8/60.0	82.4/60.4/35.9	22.8/19.2/14.1	(0.461, 0.496)	57230

[a] Operating voltage at 1, 100 and 1000 cd m^{-2}; [b] *CE*/*PE*/*EQE* = current efficiency/power efficiency/external quantum efficiency at maximum value, 100 and 1000 cd m^{-2}; [c] Commission Internationale de l'Eclairage coordinates at 1000 cd m^{-2}; [d] Maximum luminance.

thickness of TCP-BP-SFAC layer in two-color WOLEDs should be controlled within an appropriate range. A thick layer (a large x) of TCP-BP-SFAC adjacent to PPF layer will weaken the contribution of 4CzTPNBu, but a thin layer (a small x) may result in exciton accumulation and annihilation at 4CzTPNBu. The function of TCP-BP-SFAC layer adjacent to mCP layer in the sandwich configuration is also investigated. To verify the necessity of this TCP-BP-SFAC layer, double-layer devices WS1 with an EML of 1.5 wt% 4CzTPNBu: TCP-BP-SFAC (5 nm)/TCP-BP-SFAC (6 nm) and WS2 with an EML of 1.5 wt% 4CzTPNBu: TCP-BP-SFAC (14 nm)/TCP-BP-SFAC (6 nm) are fabricated for comparison (Supplementary Fig. 4 and Supplementary Tables 1 and 3). WS1 shows obviously decreased *PE* of 90.7 lm W^{-1} and *EQE* of 23.2% in comparison with W1-6. But with a thicker layer of 1.5 wt% 4CzTPNBu: TCP-BP-SFAC (14 nm), WS2 can provide comparable *PE* of 124.9 lm W^{-1} and *EQE* of 30.1% to those of W1-6. This result discloses this TCP-BP-SFAC layer can serve as a buffer layer to alleviate exciton annihilation, in addition to balance the carrier transport in the device.

All-fluorescence three-color WOLEDs

The light sources with high color rendering index (CRI) have diverse operating occasions including indoor-illumination, backlight, mirror lamp, decorative lighting, etc. The conventional fluorescence dopants have advantages of high color quality and stability, which are favorable to increase CRI of WOLEDs, but often encounter the problem of inferior EL efficiencies due to low exciton utilization. The out-of-phase sensitization system was previously demonstrated as an effective approach to sensitize conventional fluorescence dopants with reduced exciton loss for WOLEDs. Herein, a novel design of out-of-phase sensitization configuration on the basis of above sandwich configuration of two-color devices is proposed for three-color WOLEDs to have a higher CRI. Three-color white EMLs consisting of 1 wt% DBP: TCP-BP-SFAC (14 – x nm)/1.5 wt% 4CzTPNBu: TCP-BP-SFAC (x nm)/TCP-BP-SFAC (6 nm) are prepared, in which x is 5, 4 and 3 for devices W2-1, W2-2 and W2-3, respectively (Fig. 3a). Different from the sandwich configuration, one of the TCP-BP-SFAC layers is doped with red fluorescence DBP to form a red EML to improve CRI. This red EML is envisioned to be sensitized by adjacent orange EML through FET to obtain high EL efficiencies. The detailed EL performance of W2-1~W2-3 are displayed in Fig. 3b, Supplementary Fig. 5 and Table 2. The CRI is successfully increased from 65 of W2-1 to 71 of W2-3, which is close to those of normal lighting devices. Inspiringly, W2-1 achieves remarkable EL performances with a *PE* of 106.8 lm W^{-1} and an *EQE* of 30.8%. W2-2 and W2-3 also exhibit excellent EL performances, with *PE*s and *EQE*s of 99.7 lm W^{-1} and 29.1%, and 92.4 lm W^{-1} and 29.6%, respectively. Like two-color WOLEDs, these three-color WOLEDs also hold high efficiency stability. The *PE*s of W2-1, W2-2 and W2-3 are maintained at 80.6, 83.0 and 72.8 lm W^{-1} at 100 cd m^{-2}, and 52.6, 58.2 and 48.2 lm W^{-1} at 1000 cd m^{-2}, respectively, disclosing these devices are amongst the best three-color WOLEDs (Fig. 3c and Supplementary Table 4). [20,29,34-36]

To decipher the sensitization process, a supplementary device WS3 with an EML of 1 wt% DBP: mCP (5 nm)/1.5 wt% 4CzTPNBu: TCP-BP-SFAC (14 nm)/TCP-BP-SFAC (6 nm) is fabricated, which is coincident with the reported out-of-phase sensitization design (Supplementary Fig. 4 and Supplementary Tables 1 and 3).[37] WS3 shows excellent *PE* and *EQE* of 126.8 lm W^{-1} and 30.6%, respectively, but the EL spectrum of WS3 is barely changed in comparison with that of W1-6, in which the characteristic peak of DBP cannot be observed. The primary cause for the failed sensitization is the large span between the recombination zones of 4CzTPNBu and DBP, due to severe electron trapping of 4CzTPNBu as illustrated in Supplementary Fig. 3. Another supplementary device WS4 with an EML consisting of a single doped film of 1 wt% DBP: TCP-BP-SFAC (20 nm) is fabricated (Supplementary Table 1). WS4 has an *EQE* of only 4.9%, close to the *EQE* limit of the conventional fluorescence devices, indicating TCP-BP-SFAC is not a suitable sensitizer for DBP and causes severe exciton loss, namely DBP cannot be sensitized by TCP-BP-SFAC host.

Further, four doped films of 1.5 wt% 4CzTPNBu: TCP-BP-SFAC (15 nm) (film I), 1 wt% DBP: TCP-BP-SFAC (9 nm)/1.5 wt% 4CzTPNBu: TCP-BP-SFAC (5 nm) (film II), 1 wt% DBP: TCP-BP-SFAC (15 nm) (film III), and TCP-BP-SFAC (15 nm) (film IV) are prepared to study the sensitization process. As illustrated in Fig. 3d, the PL peaks of TCP-BP-SFAC, 4CzTPNBu and DBP are located at 480, 550 and 610 nm, respectively, which are consistent with their intrinsic PL properties. The transient PL decay curves detected at these PL peaks reveal that film IV has the longest decay lifetime at 480 nm (Fig. 3f and Supplementary Table 5). The mechanism of exciton behaviors is depicted in Fig. 3e. The TADF dopant 4CzTPNBu has lower lying S_1 and T_1 states than TCP-BP-SFAC, which can induce exciton diffusion towards 4CzTPNBu, thus leading to reduced delayed lifetime of TCP-BP-SFAC in film I. Film II contains red and orange layers with the identical configuration to that of white EML in W2-1. The delayed lifetime of film II at 550 nm is shortened relative to that of film I. Meanwhile, conventional fluorescence dopant DBP has a considerable decay lifetime at the scale of 20 μs, much longer than that in toluene solution, evidencing efficient FET from 4CzTPNBu to DBP. This is also supported by their overlapped absorption and PL spectra (Fig. 1b). In film III, TCP-BP-SFAC exhibits the shortest delayed lifetime, and DBP has the reduced delayed lifetime as well, reflecting non-radiative process dominates in film III due to the Dexter energy transfer between T_1 states from TCP-BP-SFAC to DBP. These findings manifest that the FET occurs between DBP and 4CzTPNBu but not between DBP and TCP-BP-SFAC.

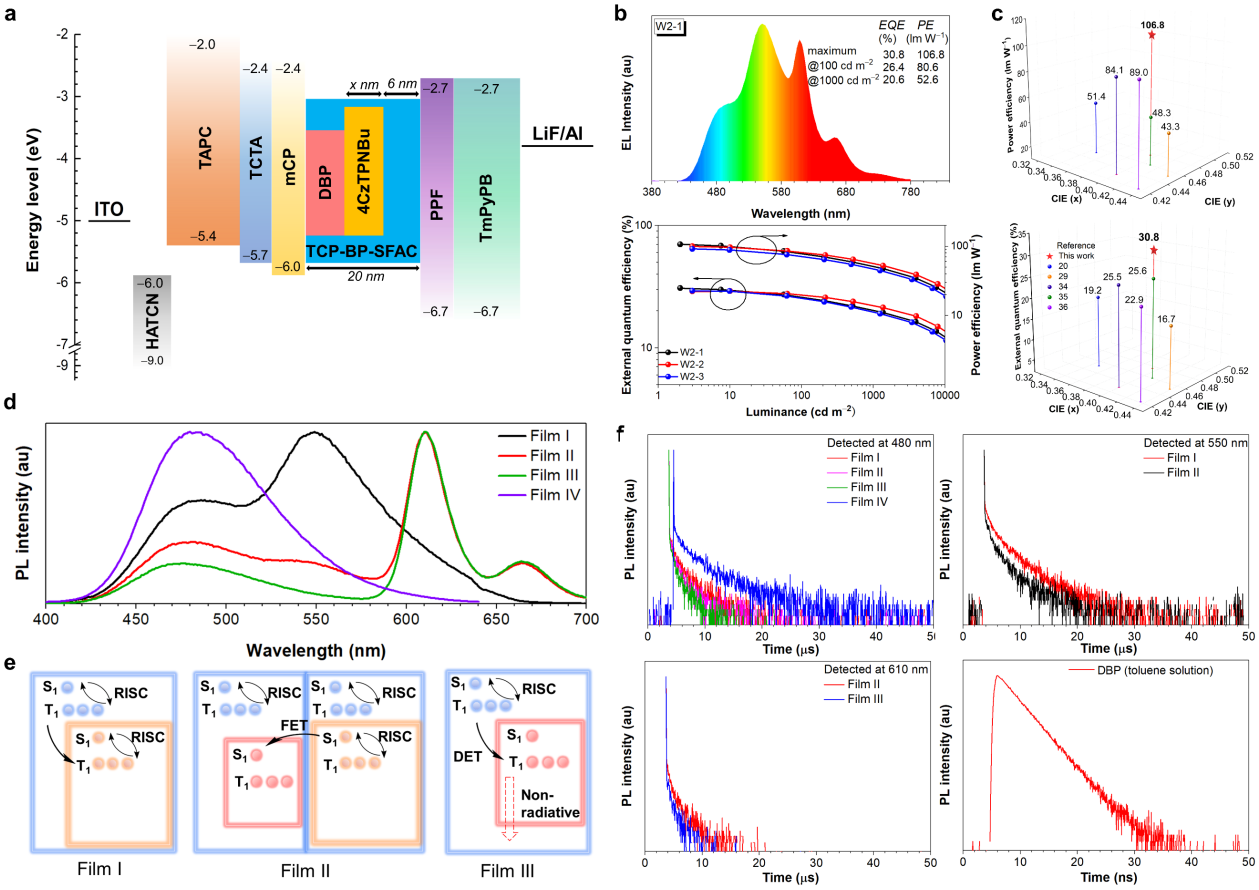

Fig. 3 **a** Device configuration of all-fluorescence three-color WOLEDs. **b** EL spectra and external quantum efficiency-luminance-power efficiency curves of W2-1~W2-3. **c** External quantum efficiency and power efficiency of representative three-color WOLEDs versus CIE coordinate. **d** PL spectra of films I~IV. **e** Mechanism illustration of exciton behaviors in films I~III. **f** Transient PL decay curves of films I~IV and DBP in toluene solution.

Host-tuning effect in WOLEDs

The photophysical results validate efficient FET from 4CzTPNBu to DBP through the out-of-phase sensitization configuration, finally producing impressive EL performance of W2-1~W2-3. To gain in-depth insights into the device mechanism, the impact from host-dopant interaction is also studied. Two typical TADF materials with close emission colors, 3,6-bis(9,9-dimethylacridin-10-yl)-xanthen-9-one (BDMAC-XT)[38] and 9-(4-(4,6-diphenyl-1,3,5-triazin-2-yl)phenyl)-9'-phenyl-9H,9'H-3,3'-bicarbazole (BCz-TRZ),[39] are selected as control hosts for comparison with TCP-BP-SFAC. The single carrier devices of BDMAC-XT and BCz-TRZ neat films and doped films with 4CzTPNBu dopant are fabricated and studied (Supplementary Fig. 2). The electron-trapping effect from 4CzTPNBu is found to be still significant in BDMAC-XT, but is less effective in BCz-TRZ, probably due to its lower lying LUMO. Three-color white EMLs with the configuration of 1 wt% DBP: Host 1 (9 nm)/1.5 wt% 4CzTPNBu: Host 2 (5 nm)/TCP-BP-SFAC (6 nm) are applied for investigation in detail (Fig. 4a). Device WS5 using BDMAC-XT as both Host 1 and Host 2 shows a low *EQE* of 23.2%, much inferior to that of W2-1 (Supplementary Fig. 6 and Supplementary Table 3). Similarly, device WS6 adopting BCz-TRZ as both Host 1 and Host 2 has a low *EQE* of 23.9% neither. Since the electron-trapping effect in BDMAC-XT is comparable to that in TCP-BP-SFAC, the low *EQE*s of WS5 and WS6 should be attributed to the efficiency decrease of 4CzTPNBu in BDMAC-XT host. As for WS6, the inefficient electron-trapping by 4CzTPNBu causes inadequate blocking of electrons, and thus exciton recombination can occur in DBP. In consequence, there is severe triplet exciton loss, resulting in a low *EQE*.

For comparison with film I (1.5 wt% 4CzTPNBu: TCP-BP-SFAC (15 nm)), films V and VI are constructed with the same configurations of 1.5 wt% 4CzTPNBu: BCz-TRZ (15 nm) and 1.5 wt% 4CzTPNBu: BDMAC-XT (15 nm), respectively. As shown in Fig. 4b, the energy levels of both S_1 and T_1 states of 4CzTPNBu are lowered progressively by doping in BDMAC-XT host to TCP-BP-SFAC host and then to BCz-TRZ host. The ΔE_{ST} values are 0.05, 0.05 and 0.11 eV for 4CzTPNBu in films I, V and VI, respectively, estimated from the fluorescence and phosphorescence spectra at 77 K (Supplementary Fig. 7), indicating TCP-BP-SFAC and BCz-TRZ are more suitable hosts than BDMAC-XT to promote RISC process and thus delayed fluorescence of 4CzTPNBu. The different ΔE_{ST} values can rationally influence the EL efficiencies of 4CzTPNBu in different hosts and consequently alter the performances of WOLEDs. Besides, the theoretical calculation is conducted for comprehensive investigation. According to the previous study, the host-tuning effect on TADF materials is virtually associated with the different polarities and the valence shell transition types of S_1 and T_1 states.[10] The natural transition orbital analysis discloses that the S_1 and T_1 states of 4CzTPNBu are dominated by π–π* transition (Supplementary Fig. 8), indicative of the similar sensitivity towards the polarity of matrix. The calculated molecular polarity index (MPI) values of S_1 and T_1 states of TCP-BP-SFAC, BCz-TRZ and BDMAC-XT are listed in Supplementary Table 6. It can be observed that BCz-TRZ has the

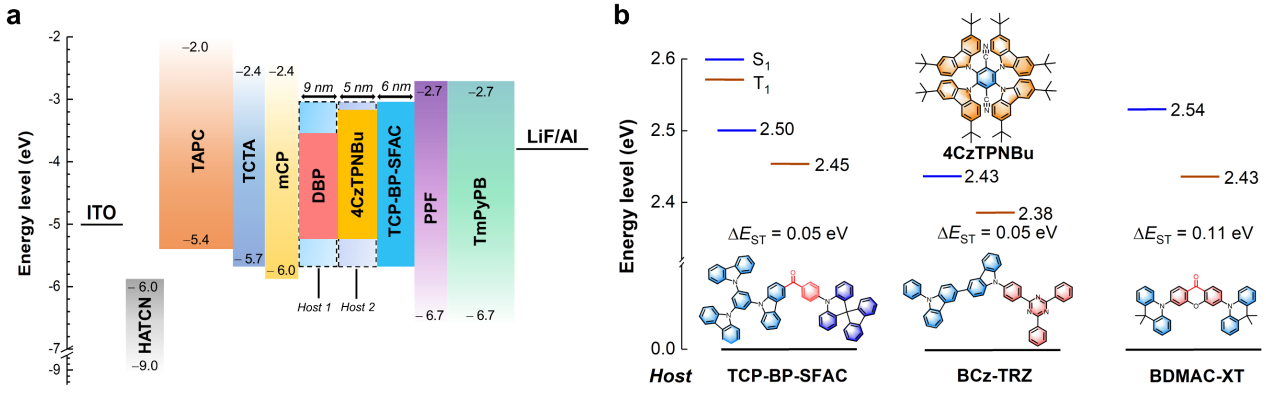

Fig. 4 **a** Device configurations of devices WS5~WS10. **b** Singlet and triplet energy levels of 1.5 wt% 4CzTPNBu in TCP-BP-SFAC, BCz-TRZ and BDMAC-XT hosts.

largest MPI values, and can lead to the lowest energy levels of S_1 and T_1 states of 4CzTPNBu, which is in good agreement with the experimental results. Such kind of host-tuning effect should be a powerful method to modulate the PL and EL behaviors of luminescent materials.

Moreover, device WS7 using BDMAC-XT as Host 1 and BCz-TRZ as Host 2 is fabricated. It exhibits sharp decrease in EL performance, with a poor *EQE* of only 13.2%. Device WS8 adopting BDMAC-XT as Host 1 and TCP-BP-SFAC as Host 2 is also prepared, which gives an *EQE* of 17.6%, higher than that of WS7. The *EQE* enhancement in WS8 mainly results from the good electron-trapping of 4CzTPNBu in TCP-BP-SFAC, which reduces the exciton recombination in DBP and thus avoids exciton loss. However, the efficiency of WS8 is still much lower than that of W2-1. Based on these findings, it is considered that the higher lying HOMO of BDMAC-XT can form relatively large hole-injection barriers between BDMAC-XT and Host 2 in WS7 and WS8. In that case, more excitons tend to recombine in DBP. Moreover, device WS9 containing an EML of BDMAC-XT (9 nm)/1.5 wt% 4CzTPNBu: TCP-BP-SFAC (5 nm)/TCP-BP-SFAC (6 nm) is fabricated. WS11 has a *PE* of 116.7 lm W^{-1} and an *EQE* of 28.2%, which are lower than those of W1-6, further confirming that the excitons are partially recombined in BDMAC-XT. In addition, WS9 using BCz-TRZ and BDMAC-XT as Host 1 and Host 2, respectively, and device WS10 using BCz-TRZ and TCP-BP-SFAC as Host 1 and Host 2, respectively, are fabricated. WS9 exhibits a *PE* of 91.6 lm W^{-1} and an *EQE* of 27.5%. WS10 shows a *PE* of 96.2 lm W^{-1} and an *EQE* of 28.9%, which are slightly better than those of WS9. From the comparison between WS9 and WS10, it is concluded that TCP-BP-SFAC is an better host for 4CzTPNBu, due to its more suitable HOMO energy levels.

Operational stability optimization

Device lifetimes are crucial parameters to evaluate to practical application potential of WOLEDs, which are greatly impacted by not only device configuration design but also the stability of the functional layers. To gain outstanding comprehensive performances by giving considerations to EL efficiencies and lifetimes of WOLEDs, preliminary device configuration optimization is conducted with commercial available functional materials at hand. Two-color device W3-1 with a configuration of ITO/MoO_3 (6 nm)/mCBP (40 nm)/1.5 wt% 4CzTPNBu: DIC-TRZ (14 nm)/20 wt% BCz-TRZ: TCP-BP-SFAC (6 nm)/TPBi (5 nm)/Bpy-TP2 (40 nm)/LiF (1 nm)/Al is prepared (Fig. 5a), in which MoO_3 is adopted as hole injection layer, 3,3′-di(9H-carbazol-9-yl)-1,1′-biphenyl (mCBP) serves as hole-transporting layer, 2, 4-diphenyl-6-bis(12-phenylindolo)[2,3-a]carbazole-11-yl)-1,3,5-triazine (DIC-TRZ) is an ambipolar host with good stability,[40] 2,2',2"-(1,3,5-benzinetriyl)-tris(1-phenyl-1-H-benzimidazole) (TPBi) is employed as hole-blocking layer, 2,7-bis(2,2'-bipyridine-5-yl)triphenylene (Bpy-TP2) works as electron-transporting layer with high stability.[41] The TCP-BP-SFAC layer is doped with BCz-TRZ to alleviate exciton quenching, and carrier injection is still kept intact under this design. The perfect carrier transport balance of DIC-TRZ and TCP-BP-SFAC[10] can play a constructive role in retarding device degradation. This device configuration actually has been greatly simplified to reduce the joule heat generation, which is conducive to prolonging device lifetimes as well.[42] W3-1 acquires warm lights and the maximum *PE* and *EQE* of 101.7 lm W^{-1} and 26.0%, respectively (Fig. 5b, Supplementary Fig. 9 and Table 1). The *PE*s are kept at 87.6 lm W^{-1} and 66.4 lm W^{-1} at 100 cd m^{-2} and 1000 cd m^{-2}, respectively, indicative of small roll-offs. The L_{max} reaches 99690 cd m^{-2}, implying the great potential to achieve high operational stability. The values of LT_{50} at initial luminance of 5000, 1700 and 700 cd m^{-2} are 61, 368 and 1927 h, respectively (Fig. 5c). At initial luminance of 100 cd m^{-2}, LT_{50} is fitted to be 56337 h. Moreover, three-color devices W3-2 and W3-3 with configurations of ITO/MoO_3 (6 nm)/mCBP (40 nm)/1 wt% DBP: DIC-TRZ (5 nm)/1.5 wt% 4CzTPNBu: DIC-TRZ (9 nm)/20 wt% BCz-TRZ: TCP-BP-SFAC (6 nm)/TPBi (5 nm)/Bpy-TP2 (40 nm)/LiF (1 nm)/Al and ITO/MoO_3 (6 nm)/mCBP (40 nm)/1 wt% DBP: DIC-TRZ (8 nm)/1.5 wt% 4CzTPNBu: DIC-TRZ (6 nm)/20 wt% BCz-TRZ: TCP-BP-SFAC (6 nm)/TPBi (5 nm)/Bpy-TP2 (40 nm)/LiF (1 nm)/Al are fabricated. W3-2 and W3-3 possess the maximum *PE*s of 97.5 lm W^{-1} and 82.4 lm W^{-1}, and *EQE*s of 24.3% and 22.8%, respectively. The *PE*s

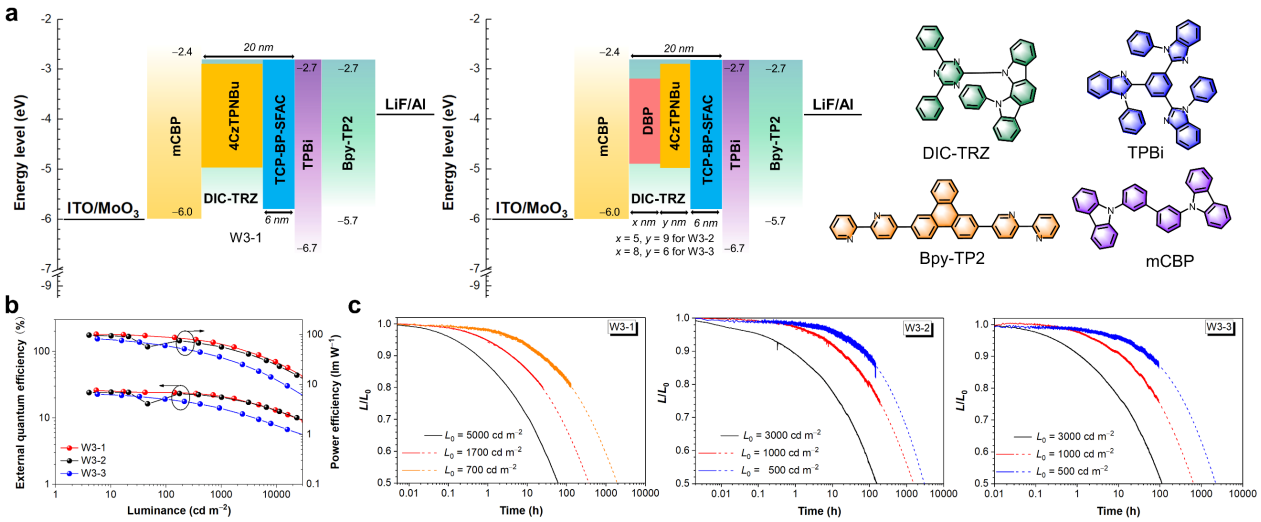

Fig. 5 **a** Device configurations of W3-1 (left), and W3-2 and W3-3 (right) with molecular structures of additional functional materials. **b** External quantum efficiency-luminance-power efficiency curves of devices W3-1~W3-3. **c** Operational lifetimes of devices W3-1~W3-3. The dashed lines are fitted from the tested values (solid lines).

of W3-2 and W3-3 are decreased moderately at operating luminance (Supplementary Fig. 9 and Table 1). The L_{max}s of W3-2 and W3-3 are 95670 and 57230 cd m^{-2}, respectively. The LT_{50} values at initial luminance of 3000, 1000 and 500 cd m^{-2} are recorded as 158, 1548 and 3029 h for W3-2, and 113, 652 and 2242 h for W3-3. The fitted values of LT_{50} at initial luminance 100 cd m^{-2} are 55335 and 31462 h for W3-2 and W3-3, respectively. The good operational stability of these devices is favored for practical application.

Conclusion

In summary, all-fluorescence two-color WOLEDs with a sandwich configuration consisting of an orange EML of delayed fluorescence 4CzTPNBu doped in delayed fluorescence TCP-BP-SFAC host located between two sky-blue EMLs of TCP-BP-SFAC neat films is proposed. Owing to the outstanding EL efficiency, small carrier injection barrier and balanced ambipolar carrier transport of TCP-BP-SFAC in neat film, the turn-on voltages of the devices are successfully lowered, and ultrahigh *PE*s and *EQE*s of up to 130.7 lm W^{-1} and 31.1% are achieved. The sandwich configuration effectively alleviates exciton quenching caused by the electron-trapping effect of 4CzTPNBu. Based on the best performed two-color device configurations, a red EML of red fluorescence DBP doped in TCP-BP-SFAC host is introduced to improve the color quality, which is sensitized by the adjacent orange EML via an out-of-phase sensitization configuration. In such device configuration, the electron-trapping effect of 4CzTPNBu can exert positive effect of preventing excitons from recombining at DBP dopant, and the FET from 4CzTPNBu greatly enhances the red emission efficiency of DBP. The generated all-fluorescence three-color WOLEDs attain remarkable *PE*s and *EQE*s of up to 106.8 lm W^{-1} and 30.8%. More importantly, both two-color and three-color WOLEDs not only acquire record-beating *PE*s but also enjoy superb efficiency stability, with much smaller *PE* roll-offs at operational luminance than those of the state-of-the-art WOLEDs. Finally, on the basis of most efficient two-color and three-color device configurations, further device optimization furnishes outstanding comprehensive performances of low driving voltages, large luminance, high EL efficiencies and long operational lifetimes for WOLEDs. The mechanism investigation demonstrates that, in addition to the suitable HOMO and LUMO energy levels, the host-tuning effect and electron-trapping effect matter significantly for realizing these high-performance WOLEDs. The design strategy for constructing highly efficient sensitization system presented in this work holds great practical potentials for the advancement of energy-conserving WOLEDs.

Methods

Materials and Instruments

The compounds HATCN, TAPC, TCTA, mCP, mCBP, PPF, TmPyPB, TPBi, Bpy-TP2, 4CzTPNBu, BCz-TRZ and DIC-TRZ were purchased from commercial sources. TCP-BP-SFAC and BDAMC-XT were synthesized according the published methods.[10, 38] PL spectra were recorded by Horiba Fluoromax-4 spectrofluorometer, and UV-visible absorption spectra were taken from a Shimadzu UV-2600 spectrophotometer. Transient PL decay curves were measured under nitrogen in a Quantaurus-Tau fluorescence lifetime measurement system (C11367-03, Hamamatsu Photonics Co., Japan).

Device fabrication and characterization

Glass substrates precoated with 90 nm ITO with resistance of 15~20 Ω per square were successively cleaned with acetone, isopropanol, detergent and deionized water in ultrasonic bath. After that, all substrates were dried in an oven maintaining at 70 °C. In order to improve the hole-injection process in WOLED devices, all substrates were treated by O_2 plasma for 10 minutes. All of the WOLED devices were fabricated by vacuum deposition method under a pressure < 5×10^{-4} Pa in the Fangsheng OMV-FS 450 vacuum deposition system. Organic materials, LiF and Al were deposited at the rates of 1~2 Å s^{-1}, 0.1 Å s^{-1} and 5 Å s^{-1}, respectively. All the devices had their luminance-voltage-current density characteristics and EL spectra measured in a PhotoResearch PR670 spectroradiometer, along with a Keithley 2400 Source Meter. The effective emitting area of the devices was 9 mm^2, determined by the overlap between anode and cathode. All the characterizations were conducted at room temperature in ambient conditions without any encapsulation, as soon as the devices were fabricated.

Theoretical calculation

The frontier molecular orbitals of TCP-BP-SFAC, 4CzTPNBu and DBP were optimized using the density functional theory (DFT) method with PBE0-D3 functional at the basis set level of 6-31G (d, p), and the natural transition orbitals of 4CzTPNBu were optimized using the time-dependent DFT method with PBE0-D3 functional at the basis set level of 6-31G (d, p). The above calculations were performed using Gaussian16 package. The MPI values, and natural transition orbital analysis were analyzed with Multiwfn.

Data availability

All the data are available from the corresponding author upon reasonable requests.

Acknowledgement

This study is financially supported by the National Natural Science Foundation of China (21788102) and the Natural Science Foundation of Guangdong Province (2019B030301003).

Author contributions

Z.Z. conceived the study experiments. H.L. designed, fabricated and measured the devices. Y.F. synthesized and characterizated the compounds and conducted the theoretical calculation. H.L. measured the photophysical property of the films. H.L. and Z.Z. wrote and revised the manuscript. Z.Z. and B.Z.T. supervised the project. All authors discussed the results and commented on the manuscript.

References

1. Kido, J., Kumura, M., Nagai, K. Multilayer White Light-Emitting Organic Electroluminescent Device. *Science* **267**, 1332-1334(1995).
2. Sun, Y., Giebink, N. C., Kanno, H., Ma, B., Thompson, M. E., Forrest, S. R. Management of singlet and triplet excitons for efficient white organic light-emitting devices. *Nature* **440**, 908-912(2006)
3. Reineke, S., Lindner, F., Schwartz, G., Seidler, N., Walzer, K., Lüssem, B., Leo, K. White organic light-emitting diodes with fluorescent tube efficiency. *Nature* **459**, 234-238(2009).
4. Uoyama, H., Goushi, K., Shizu, K., Nomura, H., Adachi, C. Highly efficient organic light-emitting diodes from delayed fluorescence. *Nature* **492**, 234-238(2012).
5. Zhang, Q., Li, B., Huang, S., Nomura, H., Tanaka, H. Adachi, C. Efficient blue organic light-emitting diodes employing thermally activated delayed fluorescence. *Nat. Photonics* **8**, 326-332(2014).
6. Tang, X., Cui, L. S., Li, H. C., Gillett, A. J., Auras, F., Qu, Y. K., Zhong, C., Jones, S. T. E, Jiang, Z.-Q., Friend, R. H., Liao, L.-S. Highly efficient luminescence from space-confined charge-transfer emitters. *Nat. Mater.* **19**, 1332-1338(2020).
7. Di, D., Romanov, A. S., Yang, L., Richter, J. M., Rivett, J. P., Jones, S., Thomas T. H., Jalebi, M. A., Friend, R. H., Linnolahti, M., Bochmann, M., Credgington, D. High-performance light-emitting diodes based on carbene-metal-amides. *Science* **356**, 159-163(2017).
8. Chen, Y. K., Jayakumar, J., Hsieh, C. M., Wu, T. L., Liao, C. C., Pandidurai, J., Ko, C.-L., Hung, W.-Y., Cheng, C. H. Triarylamine-Pyridine-Carbonitriles for Organic Light-Emitting Devices with EQE Nearly 40%. *Adv. Mater.* **33**, 2008032(2021).
9. Chen, Y., Zhang, D., Zhang, Y., Zeng, X., Huang, T., Liu, Z., Li, G., Duan, L. Approaching Nearly 40% External Quantum Efficiency in Organic Light Emitting Diodes Utilizing a Green Thermally Activated Delayed Fluorescence Emitter with an Extended Linear Donor–Acceptor–Donor Structure. *Adv. Mater.* **33**, 2103293(2021).
10. Fu, Y., Liu, H., Yang, D., Ma, D., Zhao, Z., Tang, B. Z. Boosting external quantum efficiency to 38.6% of sky-blue delayed fluorescence molecules by optimizing horizontal dipole orientation. *Sci. Adv.* **7**, eabj2504(2021).
11. Li, W., Li, W., Gan, L., Li, M., Zheng, N., Ning, C., Chen, D., Wu, Y.-C., Su, S.-J. J-Aggregation Enhances the Electroluminescence Performance of a Sky-Blue Thermally Activated Delayed-Fluorescence Emitter in Nondoped Organic Light-Emitting Diodes. *ACS Appl. Mater. Interfaces* **12**, 2717-2723(2020).
12. Ahn, D. H., Kim, S. W., Lee, H., Ko, I. J., Karthik, D., Lee, J. Y., Kwon, J. H. Highly efficient blue thermally activated delayed fluorescence emitters based on symmetrical and rigid oxygen-bridged boron acceptors. *Nat. Photonics* **13**, 540-546(2019).
13. Zhang, D., Duan, L., Zhang, D., Qiu, Y. Towards ideal electrophosphorescent devices with low dopant concentrations: the key role of triplet up-conversion. *J. Mater. Chem. C* **2**, 8983-8989(2014).
14. Wang, Q., Zhang, Y. X., Yuan, Y., Hu, Y., Tian, Q. S., Jiang, Z. Q., Liao, L. S. Alleviating efficiency roll-off of hybrid single-emitting layer WOLED utilizing bipolar TADF material as host and emitter. *ACS Appl. Mater. Interfaces* **11**, 2197-2204(2018).
15. Nakanotani, H., Higuchi, T., Furukawa, T., Masui, K., Morimoto, K., Numata, M., Tanaka, H., Sagara, Y., Yasuda, T., Adachi, C. High-efficiency organic light-emitting diodes with fluorescent emitters. *Nat. Commun.* **5**, 4016(2014).
16. Zhang, D., Duan, L., Li, C., Li, Y., Li, H., Zhang, D., Qiu, Y. High-efficiency fluorescent organic light-emitting devices using sensitizing hosts with a small singlet–triplet exchange energy. *Adv. Mater.* **26**, 5050-5055(2014).
17. Jeon, S. O., Lee, K. H., Kim, J. S., Ihn, S. G., Chung, Y. S., Kim, J. W., Lee, H., Kim, S., Choi, H., Lee, J. Y. High-efficiency, long-lifetime deep-blue organic light-emitting diodes. *Nat. Photonics* **15**, 208-215(2021).

18. Higuchi, T., Nakanotani, H., & Adachi, C. High-efficiency white organic light-emitting diodes based on a blue thermally activated delayed fluorescent emitter combined with green and red fluorescent emitters. *Adv. Mater.* **27**, 2019-2023(2015).
19. Ding, D., Wang, Z., Li, C., Zhang, J., Duan, C., Wei, Y., Xu, H. Highly Efficient and Color-Stable Thermally Activated Delayed Fluorescence White Light-Emitting Diodes Featured with Single-Doped Single Emissive Layers. *Adv. Mater.* **32**, 1906950(2020).
20. Li, X. L., Xie, G., Liu, M., Chen, D., Cai, X., Peng, J., Cao, Y., Su, S.-J. High-efficiency WOLEDs with high color-rendering index based on a chromaticity-adjustable yellow thermally activated delayed fluorescence emitter. *Adv. Mater.* **28**, 4614-4619(2016).
21. Wu, Z., Liu, Y., Yu, L., Zhao, C., Yang, D., Qiao, X., Chen, J., Yang, C., Kleemann, H., Leo, K. Ma, D. Strategic-tuning of radiative excitons for efficient and stable fluorescent white organic light-emitting diodes. *Nat. Commun.* **10**, 2380(2019).
22. Zhang, C., Zhang, D., Bin, Z., Liu, Z., Zhang, Y., Lee, H., Kwon, J. H., Duan, L. Color-tunable all-fluorescent white organic light-emitting diodes with a high external quantum efficiency over 30% and extended device lifetime. *Adv. Mater.* 2103102(2021).
23. Han, C., Du, R., Xu, H., Han, S., Ma, P., Bian, J., Duan, C., Wei, Y., Sun, M., Liu, X., Huang, W. Ladder-like energy-relaying exciplex enables 100% internal quantum efficiency of white TADF-based diodes in a single emissive layer. *Nat. Commun.* **12**, 3640(2021).
24. Chen, J. X., Wang, K., Xiao, Y. F., Cao, C., Tan, J. H., Wang, H., Fan, X.-C., Yu, J., Geng, F.-X., Zhang, X.-H., Lee, C. S. Thermally Activated Delayed Fluorescence Warm White Organic Light Emitting Devices with External Quantum Efficiencies Over 30%. *Adv. Funct. Mater.* **31**, 2101647(2021).
25. Malliaras, G. G., Scott, J. C. The roles of injection and mobility in organic light emitting diodes. *J. Appl. Phys.* **83**, 5399-5403(1998).
26. Zhang, J., Wei, Y., Xu, H. High-power-efficiency thermally activated delayed fluorescence white organic light-emitting diodes based on asymmetrical host engineering. *Nano Energy* **83**, 105746(2021).
27. Ying, S., Xiao, S., Yao, J., Sun, Q., Dai, Y., Yang, D., Qiao, X., Chen, J., Zhu, T., Ma, D. High-Performance White Organic Light-Emitting Diodes with High Efficiency, Low Efficiency Roll-Off, and Superior Color Stability/Color Rendering Index by Strategic Design of Exciplex Hosts. *Adv. Optical Mater.* **7**, 1901291(2019).
28. Ying, S., Yao, J., Chen, Y., Ma, D. High efficiency (~100 lm W^{-1}) hybrid WOLEDs by simply introducing ultrathin non-doped phosphorescent emitters in a blue exciplex host. *J. Mater. Chem. C* **6**, 7070-7076(2018).
29. Zhang, C., Lu, Y., Liu, Z., Zhang, Y., Wang, X., Zhang, D., Duan, L. A π–D and π–A Exciplex-Forming Host for High-Efficiency and Long-Lifetime Single-Emissive-Layer Fluorescent White Organic Light-Emitting Diodes. *Adv. Mater.* **32**, 2004040(2020).
30. Wu, S. F., Li, S. H., Wang, Y. K., Huang, C. C., Sun, Q., Liang, J. J., Liao, L.-S., Fung, M. K. White Organic LED with a Luminous Efficacy Exceeding 100 lm W^{-1} without Light Out-Coupling Enhancement Techniques. *Adv. Funct. Mater.* **27**, 1701314(2017).
31. Wu, Z., Yu, L., Zhao, F., Qiao, X., Chen, J., Ni, F., Yang, C., Ahamad, T., Alshehri, S. M., Ma, D. Precise exciton allocation for highly efficient white organic light-emitting diodes with low efficiency roll-off based on blue thermally activated delayed fluorescent exciplex emission. *Adv. Optical Mater.* **5**, 1700415(2017).
32. Tang, X., Liu, X.-Y., Yuan, Y., Wang, Y.-J., Li, H. C., Jiang, Z.-Q., Liao, L.-S. High-efficiency white organic light-emitting diodes integrating gradient exciplex allocation system and novel D-spiro-A materials. *ACS Appl. Mater. Interfaces* **10**, 29840-29847(2018).
33. Masui, K., Nakanotani, H., Adachi, C. Analysis of exciton annihilation in high-efficiency sky-blue organic light-emitting diodes with thermally activated delayed fluorescence. *Org. Electron.* **14**, 2721-2726(2013).

34. Liu, X. K., Chen, Z., Qing, J., Zhang, W. J., Wu, B., Tam, H. L., Zhu, F., Zhang, X.-H., Lee, C.-S. Remanagement of singlet and triplet excitons in single-emissive-layer hybrid white organic light-emitting devices using thermally activated delayed fluorescent blue exciplex. *Adv. Mater.* **27**, 7079-7085(2015).
35. Liang, J., Li, C., Zhuang, X., Ye, K., Liu, Y., Wang, Y. Novel Blue Bipolar Thermally Activated Delayed Fluorescence Material as Host Emitter for High-Efficiency Hybrid Warm-White OLEDs with Stable High Color-Rendering Index. *Adv. Funct. Mater.* **28**, 1707002(2018).
36. Ying, S., Yuan, J., Zhang, S., Sun, Q., Dai, Y., Qiao, X., Yang, D., Chen, J., Ma, D. High efficiency warm white organic light-emitting diodes with precise confinement of charge carriers and excitons in the exciplex host system. *J. Mater. Chem. C* **7**, 7114-7120(2019).
37. Liu, H., Chen, J., Fu, Y., Zhao, Z., Tang, B. Z. Achieving High Electroluminescence Efficiency and High Color Rendering Index for All-Fluorescent White OLEDs Based on an Out-of-Phase Sensitizing System. *Adv. Funct. Mater.* **31**, 2103273(2021).
38. Chen, J., Zeng, J., Zhu, X., Guo, J., Zhao, Z., Tang, B. Z. Versatile Aggregation-Enhanced Delayed Fluorescence Luminogens Functioning as Emitters and Hosts for High-Performance Organic Light-Emitting Diodes. *CCS Chem.* **3**, 230-240(2021).
39. Shizu, K., Noda, H., Tanaka, H., Taneda, M., Uejima, M., Sato, T., Tanaka, K., Kaji, H., Adachi, C. Highly efficient blue electroluminescence using delayed-fluorescence emitters with large overlap density between luminescent and ground states. *J. Phys. Chem. C* **119**, 26283-26289(2015).
40. Fukagawa, H., Ito, H., Kawamura, S., Iwasaki, Y., Inagaki, K., Oono, T., Sasaki, T., Shimizu, T. Long-Lived Efficient Inverted Organic Light-Emitting Diodes Developed by Controlling Carrier Injection Barrier into Emitting Layer. *Adv. Optical Mater.* **8**, 2000506(2020).
41. Togashi, K., Nomura, S., Yokoyama, N., Yasuda, T., Adachi, C. Low driving voltage characteristics of triphenylene derivatives as electron transport materials in organic light-emitting diodes. *J. Mater. Chem.* **22**, 20689-20695(2012).
42. Tyagi, P., Indu Giri, L., Tuli, S., Srivastava, R. Elucidation on Joule heating and its consequences on the performance of organic light emitting diodes. *J. Appl. Phys.* **115**, 034518(2014).